Chinese Chemical Letters 36 (2025) 110313

Contents lists available at ScienceDirect

Chinese Chemical Letters

journal homepage: www.elsevier.com/locate/cclet

Polydopamine-modified biochar supported polylactic acid and zero-valent iron affects the functional microbial community structure for 1,1,1-trichloroethane removal in simulated groundwater

Haitao Yin[a], Liang Meng[a,b,*], Li Li[a], Jiamu Xiao[a], Longrui Liang[a], Nannan Huang[a], Yansong Shi[a], Angang Zhao[a], Jingwen Hou[c]

[a] School of Environmental and Geographical Sciences, Shanghai Normal University, Shanghai 200234, China
[b] Yangtze River Delta Urban Wetland Ecosystem National Field Scientific Observation and Research Station, Shanghai 201722, China
[c] Instrumental Analysis Center, Shanghai Jiao Tong University, Shanghai 200240, China

ARTICLE INFO

Article history:
Received 10 June 2024
Revised 26 July 2024
Accepted 31 July 2024
Available online 2 August 2024

Keywords:
Biochar-based composite
Bioreductive dechlorination
1,1,1-TCA
Extracellular respiration microorganisms
Groundwater

ABSTRACT

In-situ enhanced bioreduction by functional materials is a cost-effective technology to remove chlorinated hydrocarbons in groundwater. Herein, a novel polydopamine (PDA)-modified biochar (BC)-based composite containing nanoscale zero-valent iron (nZVI) and poly-L-lactic acid (PLLA) (PB-PDA-Fe) was synthesized to enhance the removal of 1,1,1-trichloroethane (1,1,1-TCA) in simulated groundwater with actual site sediments. Its impact on functional microbial community structure in system was also investigated. The typical characterizations revealed uniform dispersion of PLA and nZVI particles on the BC surface, being smoother after PDA coating. The composite exhibited a significantly higher performance on 1,1,1-TCA removal (82.38%, initial concentration 100 mg/L) than Fe-PDA and PB-PDA treatments. The diversity and richness of the microbial community in the composite treatment consistently decreased during incubation due to a synergistic effect between PLLA-BC and nZVI. *Desulfitobaterium*, *Pedobacter*, *Sphaerochaeta*, *Shewanella*, and *Clostridium* were identified as enriched genera by the composite through DNA-stable isotope probing (DNA-SIP), playing a crucial role in the bioreductive dechlorination process. All the above results demonstrate that this novel composite selectively enhances the activity of microorganisms with extracellular respiration functions to efficiently dechlorinate 1,1,1-TCA. These findings could contribute to understanding the responsive microbial community by carbon-iron composites and expedite the application of *in-situ* enhanced bioreduction for effective remediation of chlorinated hydrocarbon-contaminated groundwater.

Chlorinated hydrocarbons are widely used as organic solvents. Due to their strong toxic effects and easy leakage into surrounding environments, they cause significant soil and groundwater pollution, leading to high risks to ecosystem and human health [1,2]. Therefore, research on the remediation of chlorinated hydrocarbon-contaminated groundwater is of great practical significance and application value.

Microbial dechlorination is considered as a low-cost, environmentally friendly technology to effectively remove chlorinated hydrocarbons from groundwater [3,4]. In this process, chlororespiration and dissimilatory iron reduction are two important pathways of bioreductive dechlorination, which are proceed *via* direct dechlorination through the sequential replacement of chlorines by hydrogen from microbial fermentation, and indirect dechlorination by accepting electrons from the microbially generated Fe(II), respectively [5-11]. However, the toxicity of chlorinated hydrocarbons and the complex conditions of groundwater inhibit the dechlorination capabilities of functional microorganisms, such as iron-reducing bacteria. Therefore, new approaches are needed to enhance the effectiveness of microbial dechlorination. *In-situ* enhanced bioreductive dechlorination (IEBD) technology aims to promote the biodegradation of chlorinated hydrocarbons by providing suitable nutrients and electron donors to microorganisms, attracting significant attention [12,13].

The treatment effect of IEBR is mainly determined by remedial materials, such as zero-valent iron (ZVI) and organic carbon sources [14-17]. Iron powders, especially nano ZVI (nZVI) particles exhibit quick removal of organochlorine compounds, along with simple preparation, low cost and great migration [18-21]. Beside

* Corresponding author.
E-mail address: mengliang@shnu.edu.cn (L. Meng).

https://doi.org/10.1016/j.cclet.2024.110313
1001-8417/

the directly chemical reduction by ZVI, the reduction of Fe(III) hydroxides on ZVI surface by iron-reducing bacteria can also be involved in the dechlorination of pollutants in groundwater [22]. Moreover, in actual contaminated site, the limited availability of organic carbon sources results in a low population of functional microorganisms, thus reducing their degradation capacity. Therefore, extra organic carbon sources like sodium lactate as electron donors are generally provided to increase the microbial reductive activity [23]. However, these materials face issues such as easy agglomeration and oxidation, short effective duration, and low utilization efficiency. Thus, the preparation and application of efficient functional composite materials have gradually become a new research direction.

Biochar (BC) is effective in removing chlorinated hydrocarbons from the environment due to its enriched pore structures and redox groups, enhancing absorption and microbial dechlorination [24]. Moreover, loading ZVI on BC can significantly reduce the agglomeration degree of ZVI and enhance its chemical dechlorination effect on chlorinated hydrocarbons [25]. However, the bioavailability carbon content in BC is relatively low, which cannot provide sufficient organic carbon sources for microorganisms, affecting further microbial reduction dechlorination in the long term [26]. In addition, the hydrophilicity of BC is poor, limiting its thorough contact with pollutants and microorganisms in groundwater. Poly-L-lactic acid (PLLA) can slowly release organic carbon that can be utilized by microorganisms, making it a good sustained-release carbon source [27]. Polydopamine (PDA) is rich in amine and hydroxyl groups, making it an excellent modifier to improve the antioxidant properties, hydrophilicity, and biocompatibility of base materials [28,29]. However, there are few reports on the use of PDA modified BC loading ZVI and PLLA for removing chlorinated hydrocarbons in groundwater, and indigenous microbial responses to the composite during remediation should be further explored.

This study developed a new composite of poly-L-lactic acid-supported biochar (PB)-PDA-Fe, using BC as the carrier, nZVI as the reducing agent, PLLA as the sustained carbon source, and PDA as a surface modifier. Through anaerobic microcosm cultivation, the enhanced bioreductive dechlorination effect of composite on 1,1,1-trichloroethane (1,1,1-TCA) in simulated groundwater containing actual site sediments was investigated. Furthermore, the changes in the microbial community structure in the groundwater system were analyzed using 16S rRNA high-throughput sequencing and DNA-stable isotope probing (DNA-SIP) technology to reveal key functional microbial groups responding to the composite. The meaning of this study is to offer valuable insights into the microbial response of 1,1,1-TCA degradation by this PDA-modified carbon-iron composite, thus providing the profound theoretical basis for its application in remediation of chlorinated hydrocarbon-contaminated groundwater through *in-situ* enhanced bioreductive dechlorination technologies.

The supporting information includes the process of material preparation and experimental methods. In general, composite materials formed by mechanically combining various components often have many defects. Therefore, it is necessary to organically combine the components using chemical functional modification and other means to fully leverage their advantages. This study utilized the methods of solution intercalation and liquid-phase reduction to prepare PB-PDA-Fe composite (Fig. 1a), and the X-ray diffraction (XRD) structures of the products of each component (nZVI, BC, PB, PB-PDA, PB-PDA-Fe) are shown in Fig. 1b. Specifically, nZVI exhibits distinct α-Fe^0 characteristic diffraction peaks at $2\theta = 44.8°$, 64.9°, and 82.3°, indicating that the nZVI prepared by liquid-phase reduction has a body-centered cubic structure [30]. BC and PB samples show distinct peaks of an amorphous carbon structure at $2\theta = 23.1°$ [31]. Sample PB presents a new characteristic diffraction peak at $2\theta = 16.8°$, which may be related to PLLA in the composite material [32]. Sample PB-PDA contains peaks of the amorphous carbon structure and PLLA. Sample PB-PDA-Fe exhibits all three characteristic diffraction peaks mentioned above, indicating successful loading of both PLLA and nZVI on the BC.

Further characterization was conducted using Fourier transform infrared spectroscopy (FTIR) on BC, PB, PB-PDA, and PB-PDA-Fe, with the results shown in Fig. 1c. The infrared spectrum of BC exhibits peaks mainly at 3465, 2982, 1628, 1400, 1011, 835 and 706 cm^{-1}. The broad peak near 3465 cm^{-1} corresponds to the stretching vibration of O–H; the peak near 2982 cm^{-1} corresponds to the stretching vibration of C–H; the peak near 1628 cm^{-1} corresponds to the stretching vibration of the C=C aromatic compound structure in BC; the peak near 1400 cm^{-1} may be attributed to C=O in the aromatic compound structure of BC; the peak near 1011 cm^{-1} may be related to the stretching vibration of C–O in phenols and alcohols; the peaks near 835 and 706 cm^{-1} may correspond to the vibration of C–H in the aromatic compound structure [33]. The FTIR spectrum of PB reveals peaks similar to the base material BC, with a new peak appearing near 1186 cm^{-1}, possibly due to the presence of C=O in the PLLA molecular chain, indicating successful loading of PLLA on BC. Moreover, the peak around 3465 cm^{-1} in the FTIR spectrum of PB-PDA appears broader than in PB, likely due to the overlap of stretching vibrations of hydroxyl groups on the PB surface and amine groups on the PDA membrane [34]. Lastly, a new peak at 575 cm^{-1} in the FTIR spectrum of PB-PDA-Fe corresponds to the stretching vibration of Fe–O [35], indicating successful loading of nZVI on the material with partial oxidation of the loaded nZVI.

X-ray photoelectron spectroscopy (XPS) analysis was further conducted on the surface compositions of various material samples. The three spectra lines in Fig. 1d represent the XPS full spectrum information of PB, PB-PDA, and PB-PDA-Fe. It can be observed that PB only exhibits distinct C 1s and O 1s peaks near the binding energies of 284.6 and 530.7 eV. In contrast, PB-PDA-Fe and PB-PDA, after PDA coating, not only show C 1s and O 1s peaks but also reveal a noticeable N 1s peak around 399.7 eV, indicating the presence of N 1s from PDA, thus suggesting a successful PDA coating on the material surface. In the XPS full spectrum of PB-PDA-Fe, an Fe 2p peak appears near a binding energy of 710.5 eV, which is absent in the XPS spectra of the two materials without loaded nZVI, further confirming the successful loading of nZVI on the surface of PB-PDA-Fe.

Figs. S1a and b (Supporting information) show the XPS peak spectra of elements C 1s and O 1s in PB, while Figs. S1c–f (Supporting information) display the XPS peak spectra of elements C 1s, O 1s, N 1s, and Fe 2p in PB-PDA-Fe. Fig. S1a reveals that in PB, the C 1s peaks consist of three groups: C–C/C–H (~284.6 eV, ~53.8%), C–O (~286.4 eV, ~35.4%), and O–C=O (~289.0 eV, ~10.8%), whereas the O 1s peaks only contain the C–OH/C–O (~532.6 eV, ~100%) group as shown in Fig. S1b. The results from Fig. S1c indicate that after loading of PLLA and nZVA, the C 1s peaks in PB-PDA-Fe also consist of C–C/C–H, C–O, and O–C=O groups, but with varying proportions of 50.4%, 40.4%, and 9.2% respectively. The O 1s peaks transition from a single C–OH/C–O group to a combination of C–OH/C–O (~73.0%), C=O (~531.5 eV, ~22.6%), and Fe_2O_3 (~530.2 eV, ~4.4%) groups as shown in Fig. S1d. These changes are primarily due to the introduction of new groups from PLLA, altering the types and quantities of surface groups on PB. The appearance of Fe_2O_3 in the O 1s peaks confirms the oxidation of the loaded nZVI. The N 1s peaks in PB-PDA-Fe correspond to amine-NH_2 (~401.7 eV, ~18.5%) and substituted amine-NH (~399.8 eV, ~81.5%). The transformation of amine groups in dopamine molecules to substituted amine groups indicates the occurrence of self-polymerization of dopamine with the PB matrix during the oxidation process, demonstrating the chemical encapsulation of PDA on the material surface (Fig. S1e). Analysis of the Fe

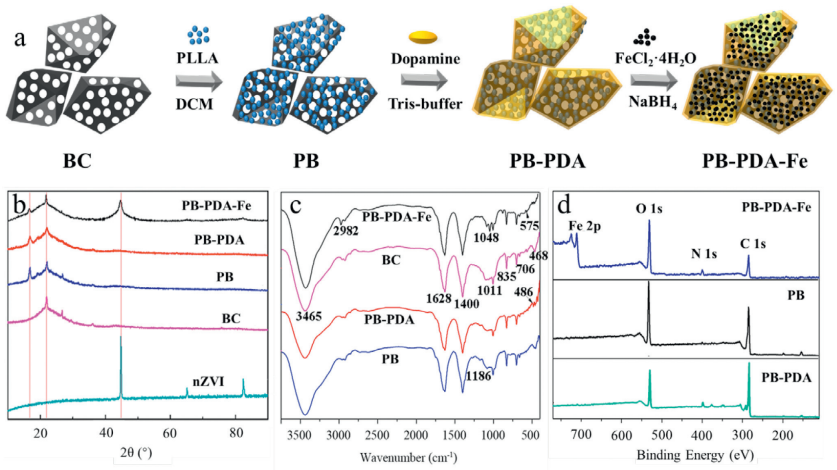

Fig. 1. (a) Schematic diagram of the preparation of PB-PDA-Fe. (b) XRD, (c) FTIR and (d) XPS spectrum of the prepared samples.

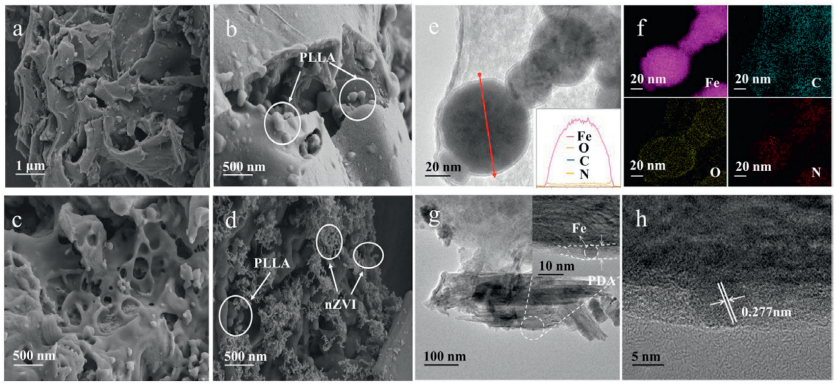

Fig. 2. SEM images of (a) BC, (b) PB, (c) PB-PDA and (d) PB-PDA-Fe. (e–h) TEM and EDS of PB-PDA-Fe.

2p peaks in PB-PDA-Fe reveals the presence of Fe(III) (~91.3%) and Fe^0 (~8.7%), with Fe(III) corroborating with the Fe_2O_3 observed in the O 1s peaks, confirming the oxidation of the loaded ZVI. Additionally, the presence of Fe^0 suggests that the oxidation is limited to the surface of the ZVI and has not further progressed (Fig. S1f) [36,37].

Figs. 2a–d illustrate the morphological structures of BC, PB, PB-PDA, and PB-PDA-Fe under scanning electron microscopy (SEM). In Fig. 2a, BC surface appears smooth with abundant and well-structured tubular pores. Fig. 2b shows PLLA irregularly dispersed as granular particles (0.5–3 μm) on the BC surface, increasing its roughness without significantly covering its pore structure. This morphology indicates that loading PLLA not only retains the original BC structure but also enhances adsorption capabilities for pollutants and microorganisms due to the increased roughness. Fig. 2c reveals that the morphology of PB-PDA is similar to PB, while PB-PDA surface is smoother due to the PDA coating. In Fig. 2d, nZVI generated through liquid-phase reduction appears as spherical particles (50–150 nm) loaded on the matrix surface, exhibiting a relatively uniform distribution with some aggregation due to its large specific surface area. Figs. 2e–h present transmission electron microscopy (TEM) and energy dispersive X-ray spectrometry (EDS) images of the composite PB-PDA-Fe. In Fig. 2e, the darker circular particles identified by EDS as nZVI have an average size of approximately 100 nm. Fig. 2f shows the EDS results indicating the main distribution of C, N, and O elements on the matrix surface, with a significant presence of O elements on the surface of nZVI particles due to their high surface area prone to oxidation. TEM observation reveals dark circular particles within the PDA coating on the material surface, with a lattice spacing of 0.277 nm matching the iron atom lattice spacing (Figs. 2g and h), suggesting the formation of smaller nZVI particles during liquid-phase reduction embedded in the PDA coating. These results are consistent with FTIR, XRD and XPS analysis.

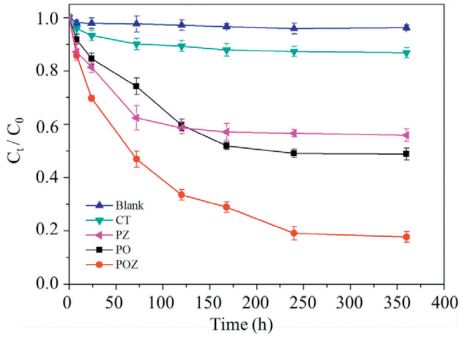

Fig. 3. Different materials were used to remove 1,1,1-TCA in simulated groundwater (C_0: initial concentration of 1,1,1-TCA; C_t: concentration of 1,1,1-TCA at time t). CT, PZ, PO and POZ represent none, Fe-PDA, PB-PDA and PB-PDA-Fe with sediment-groundwater mixture, respectively. Data are presented as mean ± standard deviation (SD) ($n = 3$).

The effects of the composite and other control materials (treatments are listed in Table S3 in Supporting information) on 1,1,1-TCA removal in simulated groundwater amended with sediments from an actual site contaminated with chlorinated hydrocarbons are shown in Fig. 3. It can be observed that in the sediment-

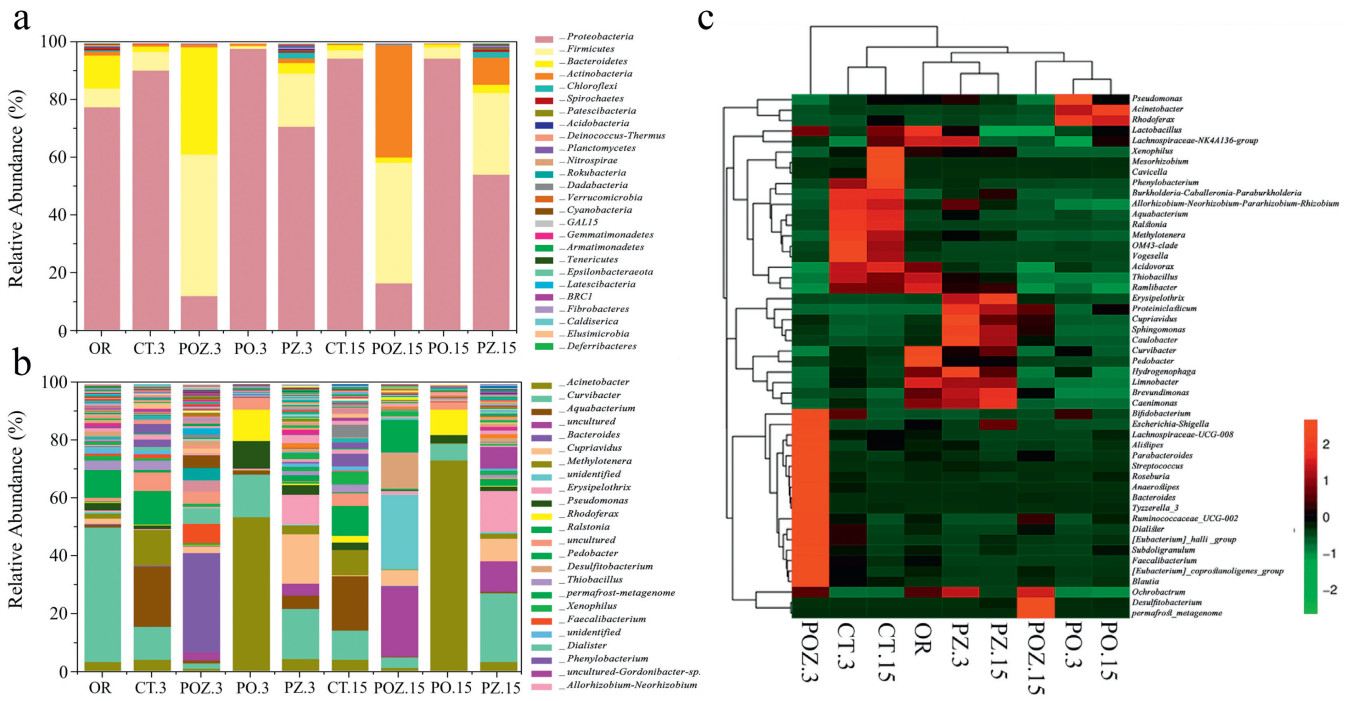

Fig. 4. Microbial distribution (a) at the phylum level and (b) at the genus level in different treatments. (c) Community composition heat map at the genus level in different treatments.

groundwater mixture (CT) treatment without adding any materials, the removal effect of 1,1,1-TCA was poor, with removal rates of 13.21% after 360 h. In contrast, in the PB-PDA-Fe + sediment-groundwater mixture (POZ) treatment with the addition of composite PB-PDA-Fe, the removal rate of 1,1,1-TCA reached 82.38% at 360 h, which was respectively 32.17% and 40.21% higher than those in the Fe-PDA + sediment-groundwater mixture (PZ) and PB-PDA + sediment-groundwater mixture (PO) treatments. This indicates that the composite material can effectively enhance the reductive dechlorination effect of 1,1,1-TCA in actual contaminated groundwater, showing potential for IEBD remediation at actual contaminated sites.

Alpha diversity is a crucial component of microbial diversity, serving as a comprehensive indicator of microbial richness and evenness within a specific region or ecosystem. Alpha diversity is primarily related to two factors: species richness and diversity, reflecting the abundance and uniformity of individuals in a community. Indices of community richness include the Chao1 and abundance-based coverage estimator (ACE). Indices of community diversity include the Shannon and Simpson. Table S4 (Supporting information) presents the Alpha diversity indices of microbial communities in different treatments in the simulated groundwater system. From Table S4, it is evident that after 3 days of incubation, both the Chao1 and ACE indices in all treatment groups decreased compared to the original sediment sample, indicating a decrease in the richness of microbial communities in sediments during the first 3-day incubation period. This decrease may be attributed to the initially high concentration of 1,1,1-TCA (100 mg/L), leading to the death of some microbes. Additionally, the reducing environment in the microbial culture system enhanced the inhibition of aerobic microbial growth present in the original sediment sample, further reducing the overall richness of microbes in the system. After 15 days of incubation, the microbial richness in CT treatment without added materials increased compared to 3 days but remained lower than the original sediment sample. While the microbial richness continued to decrease in PO, PZ, and POZ treatments with different materials added, with POZ treatment showing the most significant decrease. This indicates that the addition of these remedial materials can reduce the richness of microbes in the system. Furthermore, the Shannon and Simpson indices of microbial communities reveals that after 15 days of incubation, the diversity and evenness of microbes in treatments with different materials added also decreased. This may be due to the remedial materials promoting the growth of specific microbial communities, thereby inhibiting the growth of other pre-existing microbial communities.

Fig. 4a illustrates the distribution of dominant microorganisms at the phylum level in different treatments of the simulated system. It can be observed that the top five phyla in relative abundance in all treatments were *Proteobacteria*, *Firmicutes*, *Bacteroidetes*, *Actinobacteria*, and *Chloroflexi*. In the original sediment sample, these five phyla coexisted with abundances of 78.32%, 3.79%, 10.91%, 1.01%, and 0.32%, respectively. In CT treatment without added materials, after 3 and 15 days of cultivation, only the abundance of the *Proteobacteria* increased, while the abundances of the other phyla gradually decreased, with *Chloroflexi* not detected after cultivation. In PO treatment, the changes in microbial phylum abundance were similar to those in CT treatment, but the increase in *Proteobacteria* abundance was greater, indicating that PB-PDA promoted the growth of *Proteobacteria* in the system. In PZ and POZ treatments, the abundance of the *Proteobacteria* decreased with prolonged cultivation time, while the abundances of the *Firmicutes* and *Actinobacteria* increased. After 15 days of cultivation, the abundance of *Firmicutes* and *Actinobacteria* in POZ treatment increased by 11.2 and 38.6 times, respectively. This indicates that the nZVI component in the composite contributes to the growth of *Firmicutes* and *Actinobacteria*, inhibiting the growth of *Proteobacteria*. Studies have shown that within the *Firmicutes* and *Actinobacteria* phyla, there are various microorganisms capable of reductive dechlorination, acid-producing fermentation, and iron reduction [38,39]. Previous research has shown that a similar composite of BC-supported polycaprolactone and nZVI can synergistically enhance the removal of 1,1,1-TCA in aqueous solutions with iron reduction bacteria [40]. The changes in microbial communities at the phylum level in PZ and POZ treatments indicate that the com-

posite can also synergistically work with iron-reducing bacteria in reducing dechlorination in simulated contaminated groundwater.

Fig. 4b shows the distribution of dominant microorganisms at the genus level in different treatments of the simulated system. The dominant genera in the original sediment sample were mainly *Curvibacter*, *Pedobacter*, *Acinetobacter*, *Pseudomonas*, and *Cupriavidus*, with relative abundances of 47.78%, 9.82%, 2.21%, 1.73%, and 1.46% respectively. After 3 days of cultivation, the dominant genera in the POZ treatment system were *Bacteroides* (33.89%), *Faecalibacterium* (8.13%), and *Curvibacter* (4.31%). After 15 days cultivation, the dominant genera in the POZ system changed into *Clostridiaceasexia_uncultured* (23.79%), *OPB41_unidentified* (26.11%), *Desulfitobaterium* (10.76%), and *Pedobacter* (8.34%). *Desulfitobaterium* and *Pedobacter* are common reductive bacterial groups capable of reducing various chlorinated organic pollutants, sulfates, and nitrates [41]. The results in Fig. 4b also indicate that the relative abundance of microbial genera in the CT, PZ, and POZ treatment systems gradually became more evenly distributed with prolonged cultivation time, while in the PO system, the relative abundance of *Acinetobacter* increased with time and gradually became the most dominant genus in the system. *Acinetobacter* can produce fatty acids through fermentation of organic matters, which might further enhance the bioreduction of chlorinated hydrocarbons as electron donors [42]. They also have reductive ability to directly degrade some refractory organic pollutants by producing reductase [43]. The PO treatment system was rich in organic matters from PLLA, thus providing a favorable growth environment for *Acinetobacter* and making it become the most dominant genus. These results suggest that the various components in this composite can selectively promote the activity of functional bacterial genera, enhancing the removal efficiency of pollutants in the treatment system.

To intuitively display the abundance information of microbial community at the genus level, the community composition data at the genus level is clustered based on the abundance distribution of taxonomic units. The taxonomic units and samples are sorted according to the clustering results, and displayed in the form of a heatmap, as shown in Fig. 4c. Through clustering, it is possible to distinguish between high and low abundance taxonomic units, with the color gradient reflecting the similarity of community composition between samples. In this representation, red represents genera with higher abundance in the corresponding samples, while green represents genera with lower abundance. It can be observed that in PO treatment with the addition of PB-PDA, *Pseudomonas*, *Acinetobacter*, and *Rhodoferax* became the main genera over time. In PZ treatment with the addition of Fe-PDA, the dominant genera changed to *Erysipelothrix*, *Brevundimonas*, and *Caenimonas* over time. In POZ treatment with the addition of the composite PB-PDA-Fe, after 3 days of cultivation, the dominant genera included *Bifidobacterium*, *Escherichia-Shigella*, *Lachnospiraceae_UCG-008*, and 17 other genera. However, when the cultivation time reaches 15 days, the number of dominant genera decreased to 3, namely *Ochrobactrum*, *Desulfitobacterium*, and *Permafrost_metagenome*. Studies have shown that genera such as *Desulfitobacterium* are capable of both iron reduction and certain reductive dechlorination abilities [9,44]. This result indicates that the studied composite can preferentially promote the growth of microorganisms in the system that possess both iron reduction and reductive dechlorination abilities, further validating the synergistic effect with extracellular respiration microorganisms on 1,1,1-TCA removal in groundwater.

To assess the similarity of microbial community structures in treatments with different remedial materials, principal component analysis (PCA) was conducted on samples from each treatment. The results, depicted in Fig. 5, reveal that the first principal component axis (PC1) accounted for 54.38% of the community structure variation, while the second principal component axis (PC2)

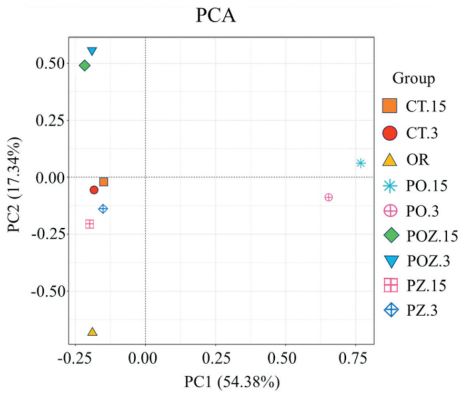

Fig. 5. PCA of microbial community structures in different treatment systems.

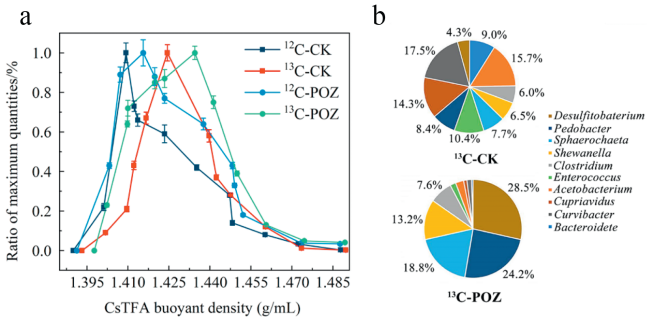

Fig. 6. (a) The quantitative distribution of 16S rRNA genes in DNA fractions obtained from ^{13}C-labeled and unlabeled treatments. (b) Diversity of microbial communities at the genus level of ^{13}C-DNA in ^{13}C-labeled treatments.

explained 17.34%, totaling 71.72%. These findings suggest distinctions in microbial community structures between CT.3 (3 days) and CT.15 (15 days) samples compared to the original sediment sample (OR) along the PC2 axis, indicating that natural substances in the sediment can influence microbial community structure. Notably, PO.3 and PO.15 samples exhibited significant differences in microbial community structure, and their microbial community structures displayed disparities on both PC1 and PC2 axes compared to OR and CT samples. Conversely, the microbial community structure in PZ.3 and PZ.15 samples only varied on the PC2 axis compared to the OR sample, and showed greater similarity to the microbial community structure of CT treatment samples. Furthermore, the microbial community structure in POZ.3 and POZ.15 samples differed significantly from both PO and PZ treatment samples. These results highlight PLLA-BC and nZVI in the composite, can alter microbial community structures in groundwater to some degrees, with the former exerting a notably higher impact. Importantly, a synergistic effect between PLLA-BC and nZVI leads to a novel selective effect on microbial community structures.

To further clarify the response of functional microorganisms in sediment-groundwater mixture to the composite, ^{13}C-labeled and unlabeled sodium acetate were added to the microcosm systems with and without PB-PDA-Fe, and the composition characteristics of the functional microbial community response to the composite in the mixture systems were analyzed after 5 days of cultivation through isopycnic density gradient ultracentrifugation and 16S rRNA high-throughput sequencing. Here, the sodium acetate was considered as the organic carbon released from the composite. After the total sediment DNA in each treated system was separated by density gradient, the quantitative analysis of bacterial DNA in each fraction with different buoyant density is shown in Fig. 6a. It can be observed that 16S rRNA gene in treatments us-

ing ^{13}C-sodium acetate as the organic carbon source (^{13}C-CK and ^{13}C-POZ) were detected in the high density DNA layer, while 16S rRNA gene in the treatments using ^{12}C-sodium acetate (^{12}C-CK and ^{12}C-POZ) were relatively enriched in the lower density DNA layer. This result indicates that bacterial DNA in the treatments with ^{13}C-sodium acetate as the organic carbon source was successfully labeled with ^{13}C and effectively separated. The compositions of dominant microorganisms at the genus level of ^{13}C-DNA in the treatments using ^{13}C-sodium acetate as the organic carbon source are shown in Fig. 6b. It can be observed that after 5 days of cultivation, the diversity of microbial communities of ^{13}C-DNA in the sediment in ^{13}C-POZ treatment did not show significant changes compared to the control treatment without added materials (^{13}C-CK), but there was a significant difference in the relative abundance of dominant microorganisms. The dominant genera present in both treatments include: *Desulfitobaterium*, *Pedobacter*, *Sphaerochaeta*, *Shewanella*, *Clostridium*, *Enterococcus*, *Acetobacterium*, *Cupriavidus*, *Curvibacter*, and *Bacteroidete*. Compared to the control treatment, the relative abundances of *Desulfitobaterium*, *Pedobacter*, *Sphaerochaeta*, *Shewanella*, and *Clostridium* in ^{13}C-POZ treatment increased by 24.2%, 13.0%, 11.1%, 6.7%, and 1.6% respectively, and these genera have been proven to possess characteristics such as iron reduction, sulfate reduction, hydrogenotrophic acidogenesis, and electroactivity, and play important roles in the bioreductive dechlorination process [45-48]. In contrast, the relative abundances of *Enterococcus*, *Acetobacterium*, *Cupriavidus*, *Curvibacter*, and *Bacteroidete*, which mainly perform carbon metabolism and energy storage functions, decreased or remained unchanged in ^{13}C-POZ treatment. These results indicate that the microorganisms in the sediment-groundwater mixture that exhibited a positive activated response to the composite were mainly reductive bacteria with extracellular electron transfer capability. They further explain that this composite mainly enhanced the activity of iron-reducing bacteria through the Fe(II)/Fe(III) system generated by Fe^0 oxidation and promoted the bioreductive dechlorination of chlorinated hydrocarbons *via* the electron shuttle capability of BC.

This study successfully prepared a novel composite with BC as the carrier, PDA as the modifier, containing PLLA and nZVI as effective components, and aimed at enhancing the bioreductive dechlorination of 1,1,1-TCA in groundwater. The results indicate that PLLA and nZVI were uniformly dispersed on the surface of biochar in granular form, and PDA modification reduced the roughness of the composite. Furthermore, this composite exhibited excellent removal efficiency for 1,1,1-TCA in simulated groundwater containing actual site sediments. The final pollutant removal rate reached 82.38%, surpassing the Fe-PDA and PB-PDA treatments by 32.17% and 40.21%, respectively. Compared to the blank control, the composite significantly reduced the diversity and richness of microbial communities in groundwater system, notably decreasing the relative abundance of *Proteobacteria*, while increasing *Firmicutes* and *Actinobacteria*. The impact of PLLA-BC in the composite on the microbial community composition was significantly larger than that of nZVI, yet both exhibited a synergistic effect, leading to a new selective effect on the microbial community. DNA-SIP analysis reveals that the enriched genera in the ^{13}C-heavy fractions in the composite treatment were associated with extracellular respiration function, playing a crucial role in the bioreductive dechlorination. In summary, this study provides a deeper understanding of the response of functional microbial communities to carbon-iron composites modified by PDA, which is contribute to the rational preparation and utilization of remedial materials to sustain key microbial activities, and ultimately improve the prospects of *in-situ* enhanced bioreductive dechlorination technologies, such as permeable reactive barrier (PRB) and *in-situ* injection, for the efficient remediation of chlorinated hydrocarbon-contaminated groundwater.

Declaration of competing interest

The authors declare that they have no known competing financial interests or personal relationships that could have appeared to influence the work reported in this paper.

CRediT authorship contribution statement

Haitao Yin: Writing – original draft, Methodology, Investigation. **Liang Meng:** Writing – review & editing, Investigation, Funding acquisition, Conceptualization. **Li Li:** Validation, Formal analysis. **Jiamu Xiao:** Methodology, Formal analysis. **Longrui Liang:** Methodology, Formal analysis. **Nannan Huang:** Validation, Software. **Yansong Shi:** Visualization, Software. **Angang Zhao:** Visualization, Software. **Jingwen Hou:** Writing – review & editing, Supervision.

Acknowledgments

This work was supported by the National Natural Science Foundation of China (No. 41877425), the Shanghai Municipal Natural Science Foundation, China (No. 21ZR1446800), the State Environmental Protection Key Laboratory of Synergetic Control and Joint Remediation for Soil & Water Pollution (No. GHBK-2022-005), the Key Lab of Eco-restoration of Regional Contaminated Environment (Shenyang University), Ministry of Education (No. KF-22-04), the Fundamental Research Funds for the Central Universities (No. 226-2022-00084), and the open fund from the Shanghai Key Lab for Urban Ecological Processes and Eco-Restoration (No. SHUES2022A04).

Supplementary materials

Supplementary material associated with this article can be found, in the online version, at doi:10.1016/j.cclet.2024.110313.

References

[1] N. Dutta, M. Usman, M.A. Ashraf, et al., Chem. Eng. J. Adv. 12 (2022) 100359.
[2] Z. Xiao, W. Jiang, D. Chen, et al., Ecotox. Environ. Safe. 202 (2020) 110925.
[3] N. Amanat, B. Matturro, M. Villano, et al., J. Environ. Chem. Eng. 10 (2022) 107047.
[4] D. Puigserver, J. Herrero, X. Nogueras, et al., Sci. Total Environ. 816 (2022) 151532.
[5] N. Wu, W. Zhang, W. Wei, et al., Chem. Eng. J. 384 (2020) 123349.
[6] Y. Sung, K.M. Ritalahti, R.A. Sanford, et al., Appl. Environ. Microb. 69 (2003) 2964–2974.
[7] L. Adrian, F.E. Löffler, Organohalide-Respiring Bacteria, Springer-Verlag, Berlin, 2016, pp. 3–6.
[8] R. Kebeish, M. Niessen, K. Thiruveedhi, et al., Nat. Biotechnol. 25 (2007) 593–599.
[9] Y. Dong, R.A. Sanford, Y. Chang, et al., Environ. Sci. Technol. 51 (2016) 232–242.
[10] L. Shi, K.M. Rosso, J.M. Zachara, et al., Biochem. Soc. Trans. 40 (2012) 1261–1267.
[11] Q. Zhang, Z. Feng, J. Zhou, et al., J. Water Process. Eng. 53 (2023) 103746.
[12] L. Zhang, L. Xu, Y. Wang, et al., Chin. Chem. Lett. 33 (2022) 4089–4095.
[13] J. Němeček, P. Pokorný, O. Lhotský, et al., Sci. Total Environ. 563 (2016) 822–834.
[14] S. Kuppusamy, T. Palanisami, M. Megharaj, et al., Rev. Environ. Contam. Toxicol. 236 (2016) 1–115.
[15] H. Chen, X. Ma, X. Zhang, et al., Chin. Chem. Lett. 34 (2023) 107701.
[16] H.J. Kim, T. Phenrat, R.D. Tilton, et al., Environ. Sci. Technol. 43 (2009) 3824–3830.
[17] Y. Wu, X. Chen, Y. Han, et al., Environ. Sci. Technol. 53 (2019) 9081–9090.
[18] R.A. Crane, T.B. Scott, J. Hazard. Mater. 211 (2012) 112–125.
[19] A.M. Zafar, M.A. Javed, A.A. Hassan, et al., Groundwater Sust. Dev. 15 (2021) 100694.
[20] H. Tang, J. Wang, S. Zhang, et al., J. Clean. Prod. 319 (2021) 128641.
[21] M. Stefaniuk, P. Oleszczuk, Y.S. Ok, Chem. Eng. J. 287 (2016) 618–632.
[22] H. Liu, T. Chen, X. Zou, et al., Chem. Eng. J. 234 (2013) 80–87.
[23] M.E. Conrad, E.L. Brodie, C.W. Radtke, et al., Environ. Sci. Technol. 44 (2010) 4697–4704.
[24] X. Chen, B. Wu, W. Yang, et al., Chem. Eng. J. 460 (2023) 141700.
[25] M. Wang, Z. Zhao, Y. Zhang, et al., J. Hazard. Mater. 403 (2021) 123972.
[26] Y. Chen, Z. Wang, K. Sun, et al., ACS ES&T Eng. 4 (2024) 603–614.
[27] C. Sun, S. Wei, H. Tan, et al., Chem. Eng. J. 446 (2022) 136881.

[28] Q. Huang, J. Chen, M. Liu, et al., Chem. Eng. J. 387 (2020) 124019.
[29] H. Li, D. Yin, W. Li, et al., Colloid. Surface B 199 (2021) 111502.
[30] Y. Xu, B.L.G.L. Zanli, J. Chen, J. Nanopart. Res. 26 (2024) 11–34.
[31] Q. Wang, S. Snyder, J. Kim, et al., Environ. Sci. Technol. 43 (2009) 3292–3299.
[32] J. Zhu, H. Cui, X. Shi, et al., Mater. Lett. 349 (2023) 134744.
[33] Z. Wang, G. Dan, R. Zhang, et al., Spectrochim. Acta A 285 (2023) 121829.
[34] B. Mao, Q. An, B. Zhai, et al., RSC Adv. 6 (2016) 47761–47770.
[35] B.Y. Yu, S.Y. Kwak, J. Mater. Chem. 20 (2010) 8320–8328.
[36] K.L. Tan, L.L. Woon, H.K. Wong, et al., Macromolecules 26 (1993) 2832–2836.
[37] Y. Long, J. Liang, Y. Xue, Environ. Sci. Pollut. R. 28 (2021) 67098–67107.
[38] G. Zeng, X. Jia, X. Zheng, et al., Environ. Sci. 35 (2014) 4244–4250.
[39] X. Zhao, Y Fan, B. Xi, et al., China Environ. Sci. 38 (2018) 3815–3822.
[40] J. Ye, Y. Mao, L. Meng, et al., Molecules 28 (2023) 3145–3160.
[41] H. Zhong, H. Lyu, Z. Wang, et al., Chemosphere 352 (2024) 141505.
[42] K. Salcedo-Vite, J.C. Sigala, D. Segura, et al., Appl. Microbiol. Biotechnol. 103 (2019) 6217–6229.
[43] P. Hongsawat, A.S. Vangnai, J. Hazard. Mater. 186 (2011) 1300–1307.
[44] D.E. Holmes, D.R. Bond, D.R. Lovley, Appl. Environ. Microbiol. 70 (2004) 1234–1237.
[45] L.C. Wunder, D.A. Aromokeye, X. Yin, et al., ISME J. 15 (2021) 3587–3604.
[46] H. Zhang, F. Liu, S. Zheng, et al., Marine Life Sci. Technol. 2 (2020) 87–96.
[47] F. Hu, B. Song, X. Wang, et al., Chin. Chem. Lett. 33 (2022) 308–313.
[48] H. Zhao, E. Su, L. Huang, et al., Chin. Chem. Lett. 33 (2022) 743–746.